



## Above-barrier surface electron resonances induced by a molecular network

R. Stiufluc,<sup>1,2</sup> L. M. A. Perdigão,<sup>3</sup> B. Grandidier,<sup>1,\*</sup> D. Deresmes,<sup>1</sup> G. Allan,<sup>1</sup> C. Delerue,<sup>1</sup> D. Stiévenard,<sup>1</sup> P. H. Beton,<sup>3</sup> S. C. Erwin,<sup>4</sup> M. Sassi,<sup>5</sup> V. Oison,<sup>5</sup> and J.-M. Debierre<sup>5</sup>

<sup>1</sup>*Département ISEN, Institut d'Electronique de Microélectronique et de Nanotechnologie (IEMN), CNRS UMR 8520, 41 bd Vauban, 59046 Lille Cedex, France*

<sup>2</sup>*Physics-Biophysics Department, Faculty of Pharmacy, University of Medicine and Pharmacy "Iuliu Hatieganu," Pasteur No. 6, Cluj-Napoca, Romania*

<sup>3</sup>*School of Physics and Astronomy, University of Nottingham, University Park, Nottingham NG7 2RD, United Kingdom*

<sup>4</sup>*Center for Computational Materials Science, Naval Research Laboratory, Washington, D.C. 20375, USA*

<sup>5</sup>*UMR-CNRS 6242, Faculté des Sciences et Techniques de Saint-Jérôme, Institut des Matériaux Nanosciences de Provence, Case 151, 13397 Marseille Cedex 20, France*

(Received 29 October 2009; revised manuscript received 10 December 2009; published 21 January 2010)

We report the modification of the density of states of the Ag/Si(111)- $\sqrt{3} \times \sqrt{3}R30^\circ$  surface by a self-assembled molecular network at energies much higher than the height of the potential barriers induced by the molecules. Map of the differential conductance obtained by scanning tunneling spectroscopy reveals an increase in the electron density in the pores of the network. This enhanced electronic resonance is explained by theoretical calculations where the periodic potential introduced by the molecular network causes band replica with an alteration of the surface band structure.

DOI: [10.1103/PhysRevB.81.045421](https://doi.org/10.1103/PhysRevB.81.045421)

PACS number(s): 73.20.At, 68.37.Ef, 81.07.Nb

### I. INTRODUCTION

The motion of an electron in a confined structure is dictated by quantum mechanics when its de Broglie wavelength becomes comparable to the dimension of the structure. As a result, the wave function of an electron trapped in a quantum well shows stationary behavior, with almost no penetration of the electron wave function beyond the potential barriers. With the advent of scanning tunneling microscopy (STM), fascinating examples of electronic standing-wave patterns on surfaces—the signature of electron localization—have been demonstrated: in semiconductor quantum dots<sup>1,2</sup> and wells,<sup>3</sup> and in nanostructures built at the surface of noble metals that exhibit Shockley-type surface states.<sup>4–9</sup>

Alternatively, electrons with energies higher than the potential barrier can be considered as unbound and propagate almost freely over the barrier. Interestingly, if the de Broglie wavelength of the electron corresponds to a half-integer multiple of its wavelength across the well,<sup>10</sup> the reflection experienced by the electron when it reaches the barrier-well interface results in an enhancement of the electron amplitude in the well. In a one-dimensional superlattice, such electronic resonances are well explained with the Kronig-Penney model and correspond to edge states at the Brillouin zone boundaries, where zone folding of the band structure occurs. With the recent advances of building two-dimensional (2D) quantum nanostructures,<sup>11</sup> it becomes possible to attain zone folding in two directions, which should allow more band mixing and greater band alteration, leading to the formation of spatial regions with enhanced electron densities. Such control of the charge distribution at the surface of a material is vital for engineering surface reactivity and may also be related to phenomena such as interface metallic conductivity or superconductivity.<sup>12,13</sup>

Band structures are generally more complex than the free-electron dispersion and the ability to enhance the density of states (DOS) above potential barriers strongly depends on

the band dispersion of the bare surface. A spectral region with high density of states is associated with a rather flat band structure. Although simple band theory predicts that the DOS can be artificially increased by periodic array of potential energy barriers, the electronic coupling between the surface and bulk states must be weak to avoid the loss of electrons into the bulk. This condition is not easily satisfied for electronic states well above the Fermi level.

Metal-induced surface reconstructions on low-index Si surfaces are rather good candidates to fulfill the latter condition. We consider here an archetypical surface reconstruction, Ag/Si(111)- $\sqrt{3} \times \sqrt{3}R30^\circ$ . Its electronic band structure exhibits a surface state band at around 2 eV above the valence band, with a large DOS. By forming molecular cavities composed of 3,4,9,10 perylene tetracarboxylic diimide (PTCDI) and 1,3,5-triazine-2,4,6-triamine (melamine) on the surface we find, in scanning tunneling spectroscopy, a modification of the DOS in this energy region. Based on *ab initio* and tight-binding calculations, we explain the occurrence of new peaks in the DOS as a consequence of the periodic structure of the molecular network, which gives rise to band folding and enhanced electron densities within the molecular cavities at energies much higher than the barrier height induced by the molecules.

### II. EXPERIMENTAL DETAILS

The surface was prepared by initially annealing the Si(111) substrate up to 1200 °C, followed by sublimation of Ag from a Knudsen cell, with the sample held at 500 °C to yield the Ag/Si(111)- $\sqrt{3} \times \sqrt{3}R30^\circ$  surface. Care was taken to minimize the concentration of Ag adatoms on top of the surface. The PTCDI and melamine were deposited under ultrahigh vacuum (UHV) conditions (base pressure <math>10^{-10}</math> Torr) by dropping grains onto a silicon sample under UHV conditions, then resistively heating to sublimate the

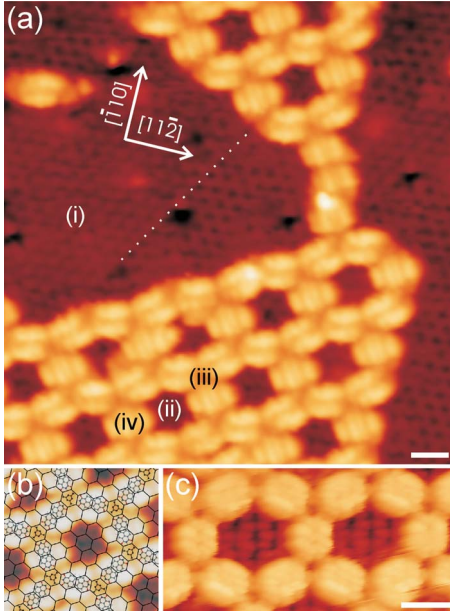


FIG. 1. (Color online) (a) STM topographic image of the PTCDI/melamine network self-assembled on the Ag/Si(111)- $\sqrt{3} \times \sqrt{3}R30^\circ$  surface ( $V_s = -2.0$  V,  $I_t = 75$  pA, and  $T = 77$  K). The dotted line indicates the position of a boundary line between two surface domains. [(i)–(iv)] Locations where the  $dI/dV$  spectra shown in Fig. 2(a) were obtained. (b) Schematic diagram of the supramolecular structure superimposed to the STM view of a pore. The hexagonal mesh represents the substrate reconstruction, with the centers of the hexagons corresponding to the silicon trimer positions. (c) High-resolution STM view of the molecular network, where the Ag/Si(111) surface reconstruction is visible in the cavities ( $V_s = -1.0$  V,  $I_t = 75$  pA, and  $T = 77$  K). Scale bar 1.5 nm.

material onto the Ag/Si sample facing the silicon heater. First, less than one monolayer of PTCDI was deposited with the Ag/Si surface held at room temperature, then followed by the deposition of melamine with the Ag/Si surface heated at  $\sim 80$  °C. Images of the surface were acquired using a low-temperature STM operating in constant-current mode. Differential conductance maps were acquired with the lock-in amplifier method ( $V_{mod} = 20$  mV<sub>p-p</sub> and  $f_{mod} = 1$  kHz), as described elsewhere.<sup>14</sup>

### III. RESULTS AND DISCUSSION

The deposition of PTCDI and melamine creates a bimolecular hexagonal network, as shown in Fig. 1 and reported in previous studies.<sup>15,16</sup> The PTCDI molecules form the edges of the hexagons and are clearly resolved. The melamine molecules are located in the vertices of the network and their central hexagonal ring appears dark. The periodicity of the network is  $3\sqrt{3}a_0 = 34.6$  Å, where  $a_0$  is the surface lattice constant of the Ag/Si(111)- $\sqrt{3} \times \sqrt{3}R30^\circ$  surface. The bimolecular arrangement is oriented with its principal axes at  $30^\circ$  relative to the  $[11\bar{2}]$  direction of the Ag/Si(111)- $\sqrt{3} \times \sqrt{3}R30^\circ$  surface,<sup>17</sup> as highlighted in Fig. 1.

The clean Ag/Si(111)- $\sqrt{3} \times \sqrt{3}R30^\circ$  surface is known to have a surface state, labeled  $S_1$ , positioned just above the

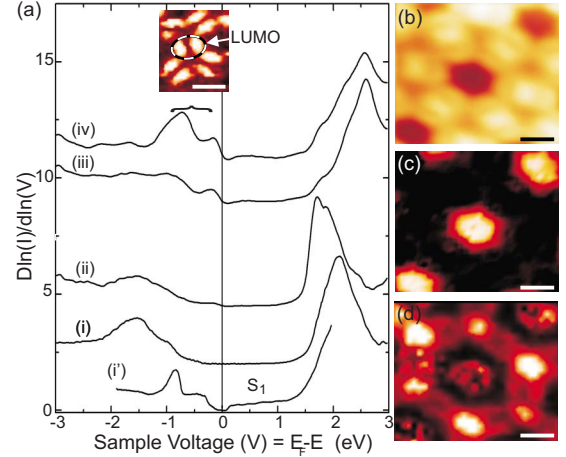


FIG. 2. (Color online) (a)  $d \ln(I)/d \ln(V)$  normalized conductance curves obtained from the average of spectra measured on the bare surface (i and i'), in the cavities (ii), on melamine molecules (iii), and on PTCDI molecules (iv) at a temperature of 77 K. The feedback conditions were sample voltage  $V_s = -3$  V and tunneling current  $I_t = 0.1$  nA, except for spectrum (i'), which was acquired at  $V_s = 2.0$  V and  $I_t = 300$  pA, with a variable tip-sample distance. The empty band of states in the Si band gap is labeled  $S_1$ . The spectra are shifted for clarity. Inset:  $dI/dV$  map with  $V_s = -0.5$  V showing the hybridized LUMO states of five PTCDI molecules. (b) STM topographic image of a cavity ( $V_s = -3.0$  V,  $I_t = 100$  pA, and  $T = 77$  K) and [(c) and (d)] simultaneously acquired  $dI/dV$  maps with  $V_s = +1.85$  V and  $V_s = +2.55$  V. Scale bar 1.5 nm.

Fermi level, with a nearly constant DOS throughout the band gap of silicon [spectrum (i') in Fig. 2], consistent with an isotropic paraboloidal energy dispersion.<sup>18,19</sup> At higher positive energies  $dI/dV$  increases sharply [spectrum (i)]; this increase is clearly resolved in inverse photoemission spectra.<sup>20</sup> This peak, at 2 eV above the top of the valence band, was initially attributed to surface states resonant with bulk states. But our calculations (below) suggest this peak is a combination of states from the top of the  $S_1$  band and Ag(*p*) orbitals.

Standing-wave patterns have already been observed for states at the bottom of the  $S_1$  band,<sup>21,22</sup> where the dispersion is free electronlike. Here we focus on higher-lying states. To determine whether the molecular network significantly modifies the DOS at higher energies, we performed spatially resolved differential conductivity measurements at constant tip-sample distances. An increase in the DOS above +1 eV is clearly seen in spectra (ii)–(iv) of Fig. 2, which arise from different tip positions as indicated in Fig. 1. (These measurements lack sensitivity below +1 eV due to the feedback conditions and the small DOS at the bottom of the  $S_1$  band.) The position and intensity of the major peak around +2 eV strongly depend on the position of the tip. In the middle of a cavity (ii), this peak has two maxima and is centered at +1.80 eV. When the tip is above the melamine (iii) and PTCDI (iv) molecules, the intensity of the single main peak is reduced and its position shifts upward by 0.47 and 0.44 eV, respectively, relative to the bare surface.

To understand the origin of these changes, we first used density-functional theory (DFT) to calculate the band structure of the clean Ag/Si(111) surface, assuming the inequiva-

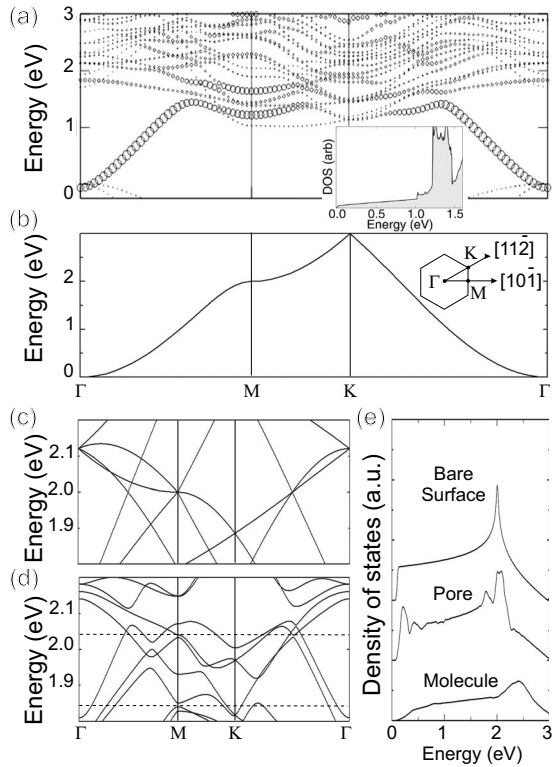


FIG. 3. (a) Band structure of the inequivalent triangle model of Ag/Si(111)- $\sqrt{3} \times \sqrt{3}$ , calculated with density-functional theory. The size of the circles denotes surface Ag character. The Fermi level is set to zero. Inset: corresponding density of surface Ag states. (b) Tight-binding band structure obtained for a simple hexagonal Ag lattice. [(c) and (d)] Detail of tight-binding band structure for a hexagonal Ag lattice covered with a hexagonal array of potential barriers representing the PTCDI and melamine molecular network. The barrier is set to zero in (c) and to 0.25 eV in (d). Dotted lines indicate energies at which several bands are clustered near the M and K points. Note that the Brillouin zone in (c) and (d) is smaller, by a factor  $3\sqrt{3} \times 3\sqrt{3}$ , than in (a) and (b); for clarity they are displayed here on the same scale. (e) Calculated density of states for the bare Ag/Si(111) surface, in the center of the molecular cavity and at the position of both types of molecules.

lent triangle model<sup>17</sup> and using DFT methods described in Ref. 23. The band structure is shown in Fig. 3(a). The state dispersing through the Si band gap arises mainly from Ag  $p$  and  $d$  orbitals at the surface. The corresponding DOS, shown in the inset, is nearly flat and thus matches well the  $S_1$  state shown in spectrum (i') of Fig. 2(a). The DFT calculations also reveal several relatively flat surface bands, centered around the M point, which form a peak in the surface DOS at 1.3 eV. This matches the observed peak near 2 eV in spectrum (i) of Fig. 2(a); the discrepancy in energy is due to the DFT underestimate of band widths, which is typically 30%.

Adsorption of the PTCDI/melamine molecular network on the clean surface leads to a significant shift of the main peak below 2 eV. Since the molecular network does not modify the Ag/Si(111) reconstruction in the pore, as seen in Fig. 1(c), and the Fermi level is pinned at the top of the valence band, preventing the tip from inducing a significant band bending at the surface, the spectroscopic changes mea-

sured in the conduction band are attributed to a modification of the surface band structure by the molecular network. As it is not computationally feasible to study such a surface comprehensively with DFT, we used a tight-binding approach to model first the clean Ag/Si surface and then the surface with the adsorbed network. Our aim is to provide the simplest model of the system in order to understand the effect of the molecules on the surface band states. In this context, it is important (1) to describe the single surface band that mostly couples to the STM tip orbitals; (2) to keep the original Bravais lattice of the surface; and (3) to mimic the effect of the molecular potential on the surface states. On the clean surface, the three Ag atoms in each  $\sqrt{3} \times \sqrt{3}$  unit cell form two inequivalent triangles. In our tight-binding model we used a single  $s$  orbital to represent each triangle. We assumed nearest-neighbor interactions only and adjusted the hopping matrix elements to best fit with the DFT surface band shown in Fig. 3(a). The resulting band matches reasonably well that of the much more complicated band structure obtained from DFT [Fig. 3(b)]. The calculated density of states shown in Fig. 3(e) is also consistent with the spectrum (i') measured on the Ag/Si(111) surface, as shown in Fig. 2(a).

The PTCDI/melamine network was modeled using square potential barriers of height  $V_0$  to represent the PTCDI and melamine molecules. In tight binding, we simply add  $V_0$  to the on-site energy of the  $s$  orbitals covered by the molecules. Because the molecular network is commensurate with the clean Ag/Si surface, the band structure in the smaller Brillouin zone is a folded (and rotated) replica of the band in Fig. 3(b), with an additional modulation due to the potential of the molecular network. For clarity, we first show the exactly folded bands in Fig. 3(c), obtained by setting  $V_0$  to zero. When  $V_0$  differs from zero, gaps appear in the band structure and modify the DOS. By setting  $V_0$  to 0.25 eV, two clusters of bands around the M and K points emerge [Fig. 3(d)]. From the comparison of the DOS obtained for the bare surface, these bands lower the overall position of the main peak and modulate its intensity through the occurrence of two small peaks, as it is seen in Fig. 3(e). The new DOS appears consistent with spectrum (ii). Although we varied  $V_0$  from tens of millielectron volt to more than 1 eV, a range of potential barriers that have been found in superlattice of atomic adsorbates built on metallic surfaces,<sup>24–26</sup> only barriers with a small height, around  $0.25 \pm 0.05$  eV allow to reproduce the shift and shape of the main peak positioned near 2 eV.

While such a barrier is high enough to confine the lowest states of the  $S_1$  band, as indicated by the oscillation of the calculated DOS in the pore that is visible in Fig. 3(e), much higher states are kept extended. But the electronic distribution of these states should, in principle, be altered. A map of the differential conductance acquired in an area where three molecular pores are visible [see Fig. 2(b)] reveals a reproducible maximum of the electron density in the cavity at a voltage of +1.85 V, as visible in Fig. 2(c). This experimental result is consistent with the calculations of the electron density that shows, in Fig. 4(b), a strong enhancement in the cavities for states within 100 meV of 1.85 eV.

At higher energies, around 2.5 eV, the contrast in the differential conductance map of Fig. 2(d) is strongly reduced in the cavities and becomes brighter at the position of the

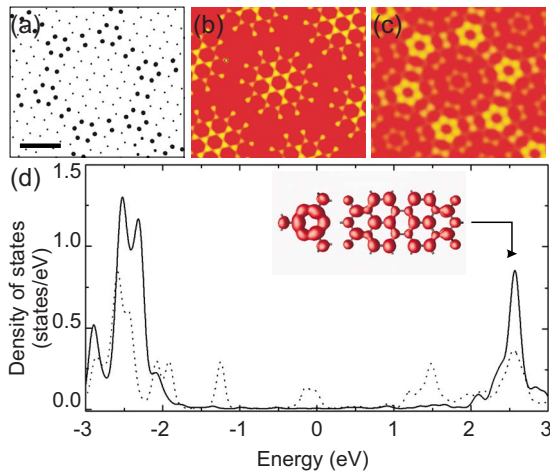


FIG. 4. (Color online) (a) Schematic model of the Ag/Si lattice showing the locations (black circles) of potential barriers used to represent the PTCDI and melamine molecules. The barrier height was set to 0.25 eV. The scale bar is 1.5 nm. [(b) and (c)] Calculated probability densities at energies of +1.9 and +2.4 eV. (d) Electronic density of states of the melamine (solid line) and PTCDI (dotted line) molecules adsorbed on the Ag/Si surface. Inset: electron-density isosurface for states between 2.57 and 2.60 eV.

melamine molecules. Within our tight-binding model there is a qualitatively similar calculated behavior for the electronic distribution of the states at 2.5 eV, as shown in Fig. 4(c). However, an increase in the electron density at the position of the molecules may also arise in part from effects not considered in our simple one-band model with square barriers. The model does not allow, for example, the possibility of additional electronic states from the adsorbed molecules. These could, in principle, also contribute to the additional peaks in the measured spectra. To investigate this possibility we performed DFT calculations of the electronic structure of adsorbed melamine and PTCDI on a Ag(111) surface, as described in Ref. 27. The lowest unoccupied molecular orbital (LUMO) of melamine and the LUMO+1 level of PTCDI are found to lie at around 2.5 eV above the Fermi level, as shown in Fig. 4(d), with the LUMO of PTCDI being positioned below the Fermi level [see inset of Fig. 2(a)], in agreement with previous experimental studies.<sup>28</sup> The positions of these levels are in good agreement with the peaks observed in spectra (iii) and (iv) of Fig. 2(a). The electron density obtained for the complex consisting of both molecules [inset of Fig. 4(d)] also resembles the contrast visible in the  $dI/dV$  map of Fig. 2(d). Thus, we conclude that the electronic waves at the cavity boundaries arise from a fortuitous combination of both effects: electronic resonances induced by potential barriers and molecular orbitals from the adsorbates.

Finally, from the DFT calculations, the atomic surface potential was determined for a bare Ag(111) surface and the Ag(111) surface after the adsorption of the molecular complex. In order to minimize the periodic potential fluctuations induced by the atomic lattices and to determine the mean potential, both potential profiles were subtracted along the main axis of the molecular complex and the result was spatially averaged in a cell with a length of 19.86 Å and a width

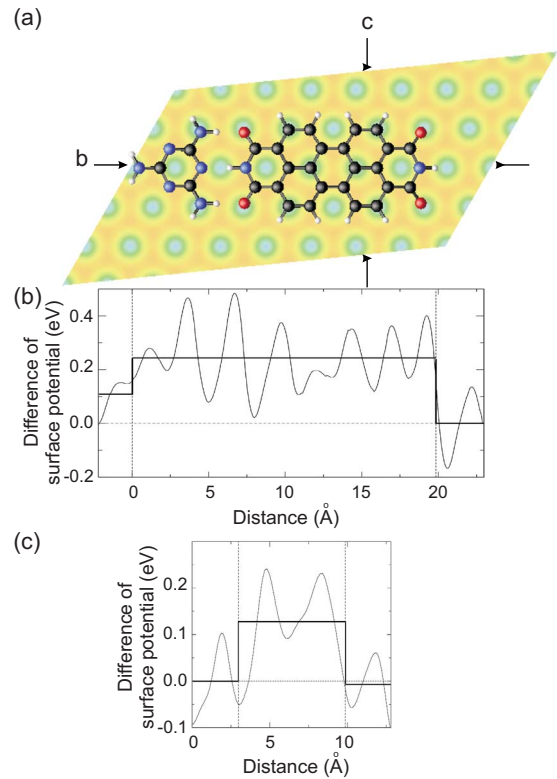


FIG. 5. (Color online) (a) Schematic diagram showing the registry of the PTCDI-melamine molecular complex with the Ag(111) surface. [(b) and (c)] Difference of the surface potential between the Ag(111) surface after the adsorption of the PTCDI/melamine complex and the bare Ag(111) surface. The potential profile has been, respectively, obtained along the main axis of the molecular complex and along a segment that runs perpendicular to this axis, as pointed out by the arrows in (a). The mean potential barrier, drawn as a strong line, has been calculated in the three regions defined by the dotted lines.

of 5.30 Å. As seen in Fig. 5, the difference of the surface potentials after and before the adsorption of the molecular complex shows that the molecules indeed act as potential barriers. The mean potential increases by 240 meV at the location of the molecules with respect to the potential calculated on the bare Ag atoms. A smaller variation of 130 meV is found in the direction perpendicular to the molecular complex but the average was obtained for a more restricted area of the bare surface. Therefore the DFT calculations yield a mean potential consistent with the one deduced from the tight-binding calculations. In both models, the Ag atoms bear a  $s$  orbital and it is the  $5s^1$  electron of the Ag atoms that give rise to the Shockley surface states of the Ag(111) surfaces. As described in Ref. 27, the  $5s$  states are involved in the charge transfer between the Ag surface and the molecular complex. This hybridization between the  $5s$  states and the LUMO of the PTCDI molecules leads to the partial filling of the LUMO after adsorption of the molecules. As the spectroscopic measurements performed on the molecular complex adsorbed on the Ag/Si(111) surface (see Fig. 2) shows that the molecular orbitals have a similar position to the one found for the Ag(111) surface, a similar hybridization should occur between the PTCDI orbitals and the Ag surface states

of the Ag/Si(111) surface. Therefore the height of the potential barrier induced by the molecular complex on the Ag/Si(111) is of the same order of magnitude than the one obtained in the case of the Ag(111) surface, supporting the existence of potential barriers much smaller than the energy of the electronic resonance of interest.

#### IV. CONCLUSION

In summary, we have found evidence that a 2D nanostructure arrays consisting of molecules alters the band structure

of a surface. Here the adsorbed molecules form a network that is commensurate with the substrate. Because this commensurability leads to zone folding and the potential barrier induced by the molecules modify the DOS, an enhancement of the electron distribution is obtained in the molecular cavities at energies much higher than the barrier height. This result offers the prospect of tailoring the electron densities of conductive substrates using a wide range of physical and chemical methods for manipulating molecular adsorbates on surfaces.

\*bruno.grandidier@isen.iemn.univ-lille1.fr

- <sup>1</sup>T. Maltezopoulos, A. Bolz, C. Meyer, C. Heyn, W. Hansen, M. Morgenstern, and R. Wiesendanger, *Phys. Rev. Lett.* **91**, 196804 (2003).
- <sup>2</sup>A. Urbieto, B. Grandidier, J. P. Nys, D. Deresmes, D. Stiévenard, A. Lemaître, G. Patriarche, and Y. M. Niquet, *Phys. Rev. B* **77**, 155313 (2008).
- <sup>3</sup>K. Suzuki, K. Kanisawa, C. Janer, S. Perraud, K. Takashina, T. Fujisawa, and Y. Hirayama, *Phys. Rev. Lett.* **98**, 136802 (2007).
- <sup>4</sup>M. F. Crommie, C. P. Lutz, and D. M. Eigler, *Science* **262**, 218 (1993).
- <sup>5</sup>J. Li, W. D. Schneider, R. Berndt, and S. Crampin, *Phys. Rev. Lett.* **80**, 3332 (1998).
- <sup>6</sup>C. Didiot, S. Pons, B. Kierren, Y. Fagot-Revurat, and D. Malterre, *Nat. Nanotechnol.* **2**, 617 (2007).
- <sup>7</sup>C. R. Moon, L. S. Mattos, B. K. Foster, G. Zelter, W. Ko, and H. C. Manoharan, *Science* **319**, 782 (2008).
- <sup>8</sup>Y. Pennec, W. Auwärter, A. Schiffrin, A. Weber-Bargioni, A. Riemann, and J. V. Barth, *Nat. Nanotechnol.* **2**, 99 (2007).
- <sup>9</sup>J. Lobo-Checa, M. Matena, K. Müller, J. H. Dil, F. Meier, L. H. Gade, T. A. Jung, and M. Stöhr, *Science* **325**, 300 (2009).
- <sup>10</sup>G. Bastard, *Wave Mechanics Applied to Semiconductor Heterostructures* (Les Editions de Physique, Paris, 1988).
- <sup>11</sup>J. V. Barth, G. Costantini, and K. Kern, *Nature (London)* **437**, 671 (2005).
- <sup>12</sup>A. Ohtomo and H. Y. A. Hwang, *Nature (London)* **427**, 423 (2004).
- <sup>13</sup>N. Reyren, S. Thiel, A. D. Caviglia, L. Fitting Kourkoutis, G. Hammerl, C. Richter, C. W. Schneider, T. Kopp, A.-S. Ruetschi, D. Jaccard, M. Gabay, D. A. Muller, J.-M. Triscone, and J. Mannhart, *Science* **317**, 1196 (2007).
- <sup>14</sup>G. Mahieu, B. Grandidier, D. Deresmes, J. P. Nys, D. Stiévenard, and Ph. Ebert, *Phys. Rev. Lett.* **94**, 026407 (2005).
- <sup>15</sup>J. A. Theobald, N. S. Oxtoby, M. A. Philipps, N. R. Champness, and P. H. Beton, *Nature (London)* **424**, 1029 (2003).
- <sup>16</sup>L. M. A. Perdigão, G. N. Fontes, B. L. Rogers, N. S. Oxtoby, G. Goretzki, N. R. Champness, and P. H. Beton, *Phys. Rev. B* **76**, 245402 (2007).
- <sup>17</sup>N. Sato, T. Nagao, and S. Hasegawa, *Surf. Sci.* **442**, 65 (1999).
- <sup>18</sup>S. Hasegawa, X. Tong, S. Takeda, N. Sato, and T. Nagao, *Prog. Surf. Sci.* **60**, 89 (1999).
- <sup>19</sup>H. Aizawa and M. Tsukada, *Phys. Rev. B* **59**, 10923 (1999).
- <sup>20</sup>J. Viernow, M. Henzler, W. L. O'Brien, F. K. Men, F. M. Leibsle, D. Y. Petrovykh, J. L. Lin, and F. J. Himpsel, *Phys. Rev. B* **57**, 2321 (1998).
- <sup>21</sup>N. Sato, T. Nagao, S. Takeda, and S. Hasegawa, *Phys. Rev. B* **59**, 2035 (1999).
- <sup>22</sup>T. Hirahara, I. Matsuda, M. Ueno, and S. Hasegawa, *Surf. Sci.* **563**, 191 (2004).
- <sup>23</sup>S. C. Erwin, *Phys. Rev. Lett.* **91**, 206101 (2003).
- <sup>24</sup>C. Didiot, A. Tejada, Y. Fagot-Revurat, V. Repain, B. Kierren, S. Rousset, and D. Malterre, *Phys. Rev. B* **76**, 081404(R) (2007).
- <sup>25</sup>F. Baumberger, T. Greber, B. Delley, and J. Osterwalder, *Phys. Rev. Lett.* **88**, 237601 (2002).
- <sup>26</sup>M. Ternes, C. Weber, M. Pivetta, F. Patthey, J. P. Pelz, T. Gi-amarchi, F. Mila, and W.-D. Schneider, *Phys. Rev. Lett.* **93**, 146805 (2004).
- <sup>27</sup>M. Sassi, V. Oison, and J.-M. Debierre, *Surf. Sci.* **602**, 2856 (2008).
- <sup>28</sup>R. Temirov, S. Soubatch, A. Luican, and F. S. Tazuz, *Nature (London)* **444**, 350 (2006).